

SPATIOTEMPORAL VARIATIONS OF SOIL MOISTURE AND GROUNDWATER LEVEL IN A SOUTH SUMATRA PEATLAND, INDONESIA DURING 2015–2018

Mokhamad Y. N. Khakim^{1*}, Akhmad A. Bama¹, Takeshi Tsuji^{2,3}

¹Universitas Sriwijaya, Jl. Raya Palembang-Prabumulih Km. 32, 30662, Indralaya, Indonesia

²Kyushu University, 744 Motooka, Nishi-ku, Fukuoka 819-0395, Japan

³University of Tokyo, 7-3-1 Hongo, Bunkyo-ku, Tokyo 113-8656, Japan

*Corresponding author: myusup_nkh@mipa.unsri.ac.id

Received: December 21st, 2021 / Accepted: April 24th, 2022 / Published: June 30th, 2022

<https://DOI-10.24057/2071-9388-2021-137>

ABSTRACT. The peat hydrological unit of the Air Sugihan River – Air Saleh River, South Sumatra, Indonesia, experienced extreme fires during the 2015 El Niño event. Restoration of 2.0 Mha degraded peatlands has been conducted since 2016. This study aims to analyze spatiotemporal variations of soil moisture content and groundwater level in this site from 2015 to 2018. The soil moisture was estimated using a multiple regression analysis method based on the Sentinel-1A and the European Center for Medium-Range Weather Forecast dataset. The groundwater level model was calculated by using linear regression between the estimated soil moisture and water level observed from field measurements. A minimum moisture content of $\sim 0.78 \text{ m}^3\text{m}^{-3}$ and a minimum groundwater depth of $\sim 0.50 \text{ m}$ below the peat surface were estimated to cause smoldering combustion. A sharp decline in the water table depth (around 1.53 m) led to a decrease in moisture content in October 2015. This month, peat fires severely burned both cultivation and protected areas having dense drainage canals and near rivers. Although there was an increasing trend in the groundwater level and moisture content in 2016, between 2017 to 2018 the water table declined to a depth of $\sim 0.7 \text{ m}$ with a corresponding moisture content of $\sim 0.25 \text{ m}^3\text{m}^{-3}$. Such decline may have led to a few peat fires which occurred in the dry season of both 2017 and 2018. We recommended that law enforcement efforts should be conducted to raise the mean annual water table to shallower depths than 0.40 m

KEY WORDS: peatland fire, soil moisture, groundwater level, restoration, remote sensing

CITATION: Khakim M.Y.N., Bama A.A., Tsuji T. (2022). Spatiotemporal Variations of Soil Moisture and Groundwater Level in a South Sumatra Peatland, Indonesia During 2015–2018. *Geography, Environment, Sustainability*, 2(15), p. 58-70
<https://DOI-10.24057/2071-9388-2021-137>

ACKNOWLEDGEMENTS: We would like to acknowledge the Ministry of Research, Technology, and Higher Education of the Republic of Indonesia for financial support through «Penelitian Dasar Unggulan Perguruan Tinggi (PDUPT)», 054/E4.1/AK.04.PT/2021 and the JSPS KAKENHI grants JP20H01997. We also thank the European Space Agency (ESA) for providing Sentinel-1 data. The authors would also like to thank the Peatland Restoration Agency for providing SESAME data. We would like to thank the two anonymous reviewers and the academic editor.

Conflict of interests: The authors reported no potential conflict of interest.

INTRODUCTION

Peatlands, a habitat for many local unique and protected species, play an essential role in ecosystem services, including carbon balance, hydrological cycle regulation, flood control, and water quality protection (Evers et al. 2017; Page et al. 2009; Wösten et al. 2006). Indonesia is home to the largest tropical peatlands (approximately 22.5 Mha) globally (A. Hooijer et al. 2010), with a thickness of up to about 12 meters and 42% of the area is covered by a peat thickness of 2 meters (A Hooijer et al. 2006). These areas act as a significant carbon sink, storing 77% of total peat and carbon deposits (Aljosja Hooijer et al. 2006).

Peatland fires are closely related to the hydrological regime as well as other factors such as human activities and the local climate. Human activity is a factor related to land use without paying attention to environmental sustainability, including logging, canal construction, and plantation development (Miettinen et al. 2013; Page et al. 2009). In addition, the main climatic factor of

the peatland fires is the amount of rainfall (Leng et al. 2019). The extreme climate due to the 2015 El Niño burnt about 850,000 ha of peatland in Sumatra and Kalimantan (Giesen and Sari 2018). Thus, a hydrological issue is an important key to restore the degraded peatland. Soil moisture and water level are important hydrological parameters to characterize peat fires caused by climate extremes.

Peatlands in Indonesia are usually located in remote and inaccessible areas with large spatial coverage. Field measurement has a limitation in spatial coverage to map peatland. Therefore, remote sensing has become a useful complementary method for monitoring and mapping the dynamics of peatland hydrology. A remote sensing technique was applied to estimate subsidence and map vegetation degradation in the study area using the Sentinel-1 dataset (Khakim et al. 2020).

The behavior of the radar backscattering signals as a function of soil moisture has been analyzed based on empirical or physical models (Baghdadi et al. 2016; Dabrowska-Zielinska et al. 2018; Dubois et al. 1995; Oh et al. 1992). The soil moisture estimation

relying on the co-polarized channels is more robust to the presence of vegetation than relying on both the cross and the co-polarized channels (Dubois et al. 1995). When the vegetation is sparse, the radar scattering is dominated by interactions with the underlying surface (Dubois et al. 1995). Several studies utilized the radar backscattering from Sentinel-1 to estimate soil moisture with reasonable accuracy, such as over wetlands using regression models (Dabrowska-Zielinska et al. 2016; Gangat et al. 2020) and a water cloud model (Dabrowska-Zielinska et al. 2018). Meanwhile, a low correlation between water levels and radar backscattering was investigated (Asmuß et al. 2019). Other studies on the estimation of water levels were performed by using the coherence data (Chen et al. 2020; Kim et al. 2017). However, the interferometric coherence was mainly dependent on the temporal baseline and landcover types for Sentinel-1. The coherence is commonly low for wetlands; thus, it is more difficult to map water levels with reasonably spatial distribution.

This study aims to analyze spatiotemporal variations of (1) soil moisture content and (2) groundwater level at the peat hydrological unit of the Air Sugihan River – Air Saleh River, namely the Kesatuan Hidrologi Gambut Sugihan Saleh (KHGSS), South Sumatra, Indonesia, using a multiple regression analysis (MRA) method based on Sentinel-1 and ECMWF datasets. Moreover, this study aims to provide a better understanding of the variation of these two hydrological parameters during the 2015 El Niño event and three years after, during which rewetting measures were in place.

MATERIALS AND METHODS

Study area

The peat hydrological unit of the Air Sugihan River – Air Saleh River (KHGSS) is one of the tropical peatlands in South Sumatra, Indonesia (Fig. 1). This area is located between Air Sugihan River in the East and Air Saleh River in the West. This site area experienced severe fires, large subsidence, and high vegetation degradation from the 2015 El Niño phenomenon (Khakim et al. 2020).

For restoring the degraded peatland due to the 2015 peatland fires, the National Peatland Restoration Agency (BRG) was established by Presidential Decree in January 2016 (President of Republic of Indonesia 2016a). The decree mandated BRG to coordinate and facilitate the restoration of 2.0 Mha of the degraded peatland in 5 years (2016–2021). The restoration was applied in this study area through three approaches (3R), i.e., Rewetting, Revegetation, and Revitalization of livelihoods in the peatland restoration efforts (Giesen and Sari 2018).

A main purpose of rewetting is to restore hydrological properties of drained peatlands. In the study area rewetting has been conducted by blocking canals to raise groundwater levels. Besides preventing peat soil oxidation and reducing carbon emission, the rewetting has been also intended to minimize further subsidence and to prevent peat fire.

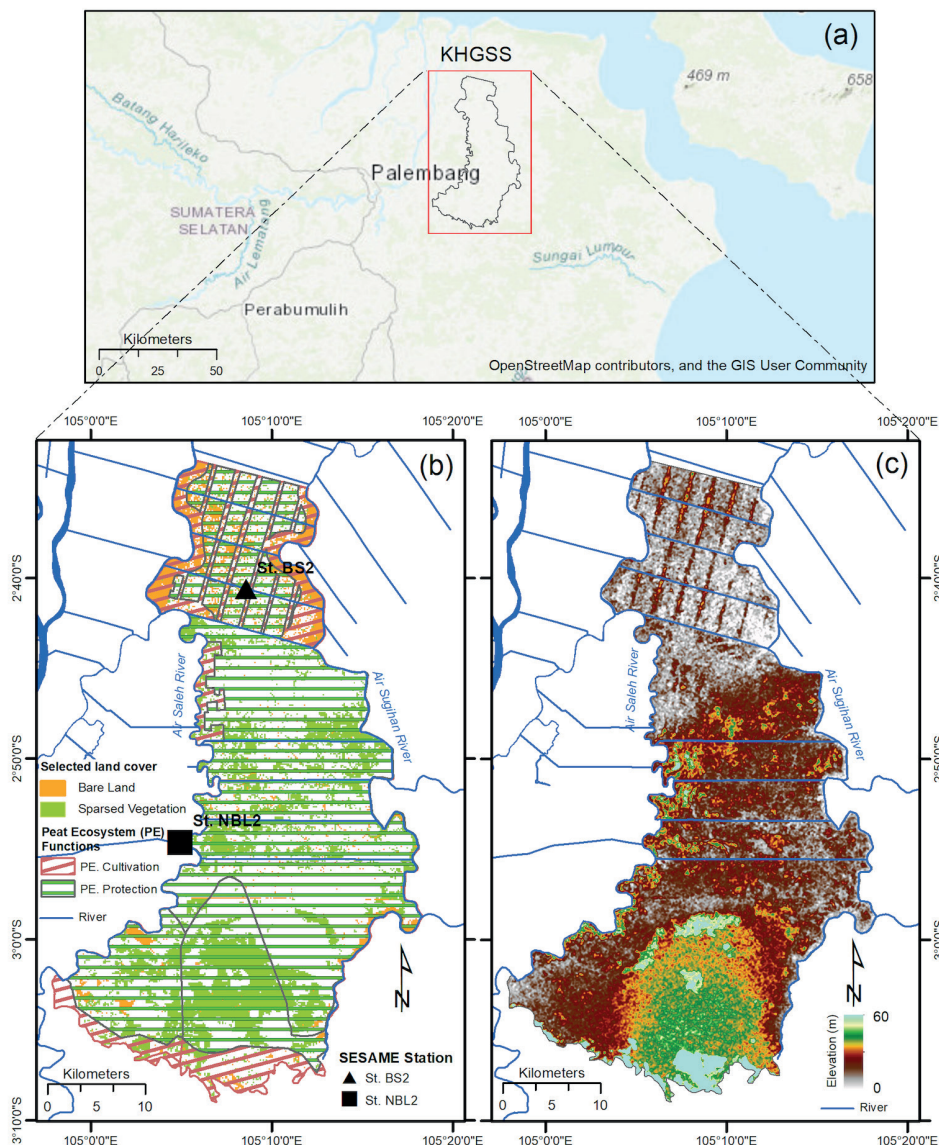


Fig. 1. (a) Location of the study area with (b) peat ecosystem functions (Peat Restoration Agency 2017) and (c) topography of the study area downloaded from <http://tides.big.go.id/DEMNAS/>

In addition, revegetation, which is the second approach of the restoration, has been intended to restore degraded peat swamp vegetation cover and improve peat forest habitat quality (Dohong 2019). The revegetation in the study area was conducted by replanting indigenous local tree species such as Jelutung (*Dyera lowii* Hook.F), Meranti Bunga (*Shorea leprosula* Miq), Meranti Batu (*Shorea platycarpa* Heim), Tanaman Sagu (*Metroxylon rumphii*), and Gelam (*Melaleuca spp*) (Sodikin et al. 2017). These local trees have been combined with pineapple in an Agroforestry pattern.

The revitalization of local livelihoods, which is the third approach, provides livelihood alternatives for local communities. Therefore, it can create various livelihood alternatives for increasing their income and welfare. Moreover, the local people can be involved in operating and maintaining canal blocking built in their respective sites (Dohong 2019). The fishery canal was made to provide their additional economic benefit. This fishery aims to cultivate species of local fish.

Data

Sentinel-1A GRD data. The European Space Agency's (ESA) Sentinel-1 constellation provides continuous global all-weather, day-and-night radar imaging with a C-band Synthetic Aperture Radar (SAR) instrument operating at a center frequency of 5.405 GHz in support of Global Monitoring for Environment and Security (GMES) applications (Attema et al. 2008). The Sentinel-1 satellite constellations have a revisit time of six days for the SAR data acquisition (Filipponi 2019). This study utilized Level 1 Interferometric Wide Swath (IW) multi-looked Ground Range Detected (GRD) products in high resolution of 20 x 22 m and a pixel spacing of 10 x 10 m (Hornáček et al. 2012). These GRD images are multi-looked with the number of looks of 5 and 1 in range and azimuth, respectively. To cover an area of interest from 2015 to 2018, we selected four datasets with different paths and frames that were downloaded from Alaska Satellite Facility (ASF), as presented in Table 1.

Table 1. The IW GRDH Sentinel-1A images used in this study

No.	Date (yyyy/mm/dd)	Path/Frame	Polarization
1	2015/01/04	98/1171	VV
2	2015/02/21	98/1171	VV
3	2015/03/17	98/1171	VV
4	2015/04/10	98/1171	VV
5	2015/05/17	120/604; 120/598	VV+VH
6	2015/07/15	98/1171	VV
7	2015/08/08	98/1171	VV
8	2015/10/19	98/1171	VV
9	2015/11/25	120/604; 120/598	VV+VH
10	2015/12/19	120/604; 120/598	VV+VH
11	2016/01/12	120/604; 120/598	VV+VH
12	2016/02/05	120/604; 120/598	VV+VH
13	2016/03/24	120/604; 120/598	VV+VH
14	2016/04/17	120/604; 120/598	VV+VH
15	2016/05/11	120/604; 120/598	VV+VH
16	2016/07/22	120/604; 120/598	VV+VH
17	2016/08/15	120/604; 120/598	VV+VH
18	2016/10/02	120/604; 120/598	VV+VH
19	2016/11/19	120/604; 120/598	VV+VH
20	2016/12/13	120/604; 120/598	VV+VH
21	2017/02/22	98/1170	VV+VH
22	2017/03/06	98/1170	VV+VH
23	2017/03/18	98/1170	VV+VH
24	2017/04/23	98/1170	VV+VH
25	2017/05/29	98/1170	VV+VH

26	2017/06/22	98/1170	VV+VH
27	2017/07/04*	98/1170	VV+VH
28	2017/08/21*	98/1170	VV+VH
29	2017/09/14*	98/1170	VV+VH
30	2017/10/20*	98/1170	VV+VH
31	2017/11/13*	98/1170	VV+VH
32	2017/12/31*	98/1170	VV+VH
33	2018/01/12*	98/1170	VV+VH
34	2018/02/17*	98/1170	VV+VH
35	2018/03/13*	98/1170	VV+VH
36	2018/04/18*	98/1170	VV+VH
37	2018/05/12*	98/1170	VV+VH
38	2018/06/17*	98/1170	VV+VH
39	2018/07/11*	98/1170	VV+VH
40	2018/08/16*	98/1170	VV+VH
41	2018/09/09*	98/1170	VV+VH
42	2018/10/03*	98/1170	VV+VH
43	2018/11/20*	98/1170	VV+VH
44	2018/12/26*	98/1170	VV+VH

*used for MRA analysis

ECMWF dataset. ERA-Interim is a global atmospheric reanalysis product from the European Centre for Medium-Range Weather Forecasts (ECMWF) that has been available since 1 January 1979 (Dee et al. 2011). This study utilized the ERA interim-daily datasets of soil moisture level-1 (0 – 7 cm), total precipitation, soil temperature level-1 (0 – 7 cm), and surface roughness in a NetCDF format downloaded from the ECMWF Data Server. We used these data with a spatial resolution of 0.125 x 0.125 degrees.

SESAME's field data. SENSory data transmission Service Assisted by Midori Engineering (SESAME), a real-time telemetry technology that records precipitation, air temperature, and groundwater level every 10 minutes, was installed in this area to monitor the effectiveness of rewetting activities (Republic of Indonesia 2018). Two stations were installed in this area, namely St. NBL2 and St. BS2. A moisture sensor was installed at a depth of 10 cm from the peat surface. While a waterproof, immersion-type sensor for water level (WL) measurement was placed in a plastic pipe installed vertically from the peat surface to the depth of the mineral soil (Republic of Indonesia 2018; Sulaiman et al. 2017).

Fire hotspot data. This study used the NASA Near Real-Time VNP14IMGTDL_NRT VIIRS 375 m Active Fire Detections in the shapefile format from January 2015 to December 2018 downloaded from the NASA earth data website <https://earthdata.nasa.gov/earth-observation-data/near-real-time/firms/>. The hotspot data from the VIIRS product has a higher resolution (375 m with nominal temporal resolutions every 12 h) than MODIS data (1 km) so it provides a more reliable estimate of fire perimeters. With this data, the spatiotemporal distribution of burnt areas can be identified. The VIIRS 375 m data are comprised

of five distinct single-gain channels extending from the visible to thermal infrared spectral region. The fire detection algorithms were based on the differential radiometric response of high-temperature targets imaged in those two spectral regions (Schroeder et al. 2014). This study used the fires with nominal and high confidence levels.

METHODOLOGY

Backscattering coefficient processing

The co-polarization (VV) GRD images from Sentinel-1 were processed into backscatter coefficients, σ^0 , in decibels. This GRD image data processing to obtain the backscatter coefficient in each pixel was implemented using the Sentinel-1 Toolbox. Workflow for processing Copernicus Sentinel-1 GRD products included orbit metadata updates, thermal and image border noise removal, radiometric calibration, as well as range-Doppler and terrain correction (Aukema and Wilson 2019; Filipponi 2019).

Orbital metadata, generally inaccurate within the SAR product, was updated using a precise orbit downloaded automatically on Sentinel Application Platform (SNAP) software version 7.0 to provide accurate information on satellite position and speed. After applying a precise orbit, thermal noise was removed to reduce the effect of noise in the image between sub-swaths; particularly, normalizing the backscatter signal in all Sentinel-1 scenes and reducing discontinuity between sub-plots for scenes in multi-swath acquisition mode. Radiometric artifacts at the image border are produced by azimuth and range compression when generating level-1 products. We then converted digital pixel values to radiometrically calibrated SAR backscatter.

This calibration also converted image intensity values into sigma naught values. The information required to apply the calibration equation is included within the Sentinel-1 GRD product; specifically, a calibration vector included as an annotation in the product allows simple conversion of image intensity values into sigma naught values. Interference of waves reflected from many elementary scatters resulted in speckles in SAR images. We multilooked the images by a factor of 6 in range and azimuth and applied multitemporal speckle filtering to reduce speckles. Our study required multiple SAR data for temporal analysis. Therefore, we stacked these SAR data before applying the multitemporal speckle filtering with the type of Lee filter (Lee 1981). Some distortions related to side-looking geometry in the SAR data were compensated for representing the image as close as possible to the real world by using range doppler terrain correction. This correction used the one arcsec NASA's Shuttle Radar Topography Mission – Digital Elevation Model (SRTM – DEM) to derive the precise geolocation information and obtain local incidence angles. The target coordinate reference system is the UTM zone 48S. Finally, the backscatter coefficient was converted to dB using a logarithmic transformation (Filipponi 2019; Xianlong Zhang et al. 2021).

Soil moisture and water level estimation

To obtain soil moisture (SM), this study applied an empirical method by using multiple linear regression analysis between backscatter coefficient, σ_{wv} (BS), local incidence angle, θ (LIA), soil moisture level-1, 0 – 7 cm, (SM), total precipitation (TP), soil temperature level-1, 0 – 7 cm, (ST), and surface roughness (SR). The backscattering coefficient and local incidence angle are variables derived from the Sentinel-1 IW level-1 GRD products, while SM, TP, ST, and SR are variables obtained from ECMWF with a spatial resolution of 0.125 x 0.125 degrees. The ERA interim-daily SM (layer 1: 0 – 7 cm), TP, ST, and SR from ECMWF were on the same date as those of the BS and LIA from Sentinel-1.

The multiple linear regression analysis refers to a technique for studying the linear relationship among two or more variables. We assumed a linear relationship between SM and independent variables (BS, LIA, TP, ST, and SR). This analysis estimated weighting factors (a-e) and the intercept (f) from Equation (1).

$$SM = a.BS + b.LIA + c.TP + d.ST + e.SR + f \quad (1)$$

For MRA analysis, values of these variables were extracted from the images located at the St. NBL2 point of the SESAME measurement station. Therefore, the predicted SM was validated using the SM measured by the SESAME station. Because SESAME data was available at this site starting around early 2017, SM from this measurement for July 2017 - December 2018 was applied to validate the predicted SM. Another SESAME station (namely St.BS2) was used to validate the predicted results in another place from the derived empirical model.

The predicted soil moisture derived from the multiple linear regression can be written as in Equation (2).

$$SM = 0.009 * BS + 0.010 * LIA + 0.206 * TP - 0.014 * ST + 0.002 * SR + 0.424 \quad (2)$$

The images of BS, LIA, TP, ST, and SR were resampled into 150 x 150-m pixel sizes to the derived spatial distribution of SM maps. Fig. 2a-e shows the correlation between variables where the highest coefficient of determination (R^2) (0.925) is the relationship between SM and TP. The result shows that the SM increased with an increase in TP. In contrast,

SM linearly decreased by increasing the surface roughness with a coefficient of determination of 0.739. A normal probability plot of sample percentiles versus predicted value (Fig. 2f) showed that the model met the assumption of normality.

The predicted soil moisture was compared with the observed soil moisture using the coefficient of determination (R^2), and unbiased root mean squared error (ubRMSE). This ubRMSE was calculated using Equation (3) (Li et al. 2018; Xuefei Zhang et al. 2017). The coefficient of determination and ubRMSE are 0.83 and 0.148 m^3m^{-3} , respectively (Fig. 2g).

$$ubRMSE = \sqrt{\frac{\sum_{i=1}^n (Obs_i - Pre_i)^2}{n} - \left(\frac{\sum_{i=1}^n (Obs_i - Pre_i)}{n} \right)^2} \quad (3)$$

As the level of soil moisture values from ECMWF data and SESAME measurements are different, the SM obtained from Equation (2) was adjusted by using the linear equation relationship between the ECMWF's SM and the SESAME's SM shown in Fig. 3a resulting in an adjusted SM as expressed in Equation (4).

$$Adj\ SM = 9.168 * SM - 2.191 \quad (4)$$

Furthermore, the linear relationship between SM and WL from SESAME measurements in the KHGSS, as shown in Fig. 3b was applied to estimate WL relative to the ground surface using Equation (5) from the adjusted SM.

$$WL = 1.497 * Adj\ SM - 1.676 \quad (5)$$

RESULTS AND INTERPRETATION

Groundwater level validation

For validation, the estimation results for groundwater level are compared to in-situ SESAME's measurement at BL2, and the level profiles are shown in Fig. 4a. The coefficient of determination and unbiased root mean squared error for the predicted water levels are 0.6119 and 0.1551 m, respectively (Fig. 4b). Based on the coefficient and error calculation, the soil moisture and groundwater level could be predicted for this study.

Relationship between fire hotspots and volumetric moisture contents

Fig. 5 shows spatial and temporal variations in soil moisture contents estimated by using Sentinel-1 and ECMWF data. These maps are overlaid with drainage networks that were created by the Indonesian Peat Restoration Agency (Peat Restoration Agency 2017). The networks were made using Lidar-derived DEM and aerial photographs with a density of 4 points/ m^2 and accuracy of less than 10 cm. In addition, Indonesian Center for Agricultural Land Resources Research and Development has created a peat thickness map with 4 classes, i.e., very thin (< 50 cm), thin (50 – 100 cm), medium (100 – 200 cm), and thick (200 – 300 cm) (BBSDL 2019). Distributions of fire hotspots were correlated with soil moisture contents. The highest moisture was detected over the site area in May 2015. The soil moisture sharply dropped up to 0.02 m^3m^{-3} starting from July to October 2015. Fire hotspots were generally associated with areas of low moisture. The lower the soil moisture, the higher the vulnerability of peatlands to fires. In 2015, the lowest moisture content of soil occurred in October. Therefore, the highest number of fire hotspots were observed this month. It indicates that the El Niño caused dry spells which in turn led to a lack of soil moisture and that in turn increased the number of fire hotspots.

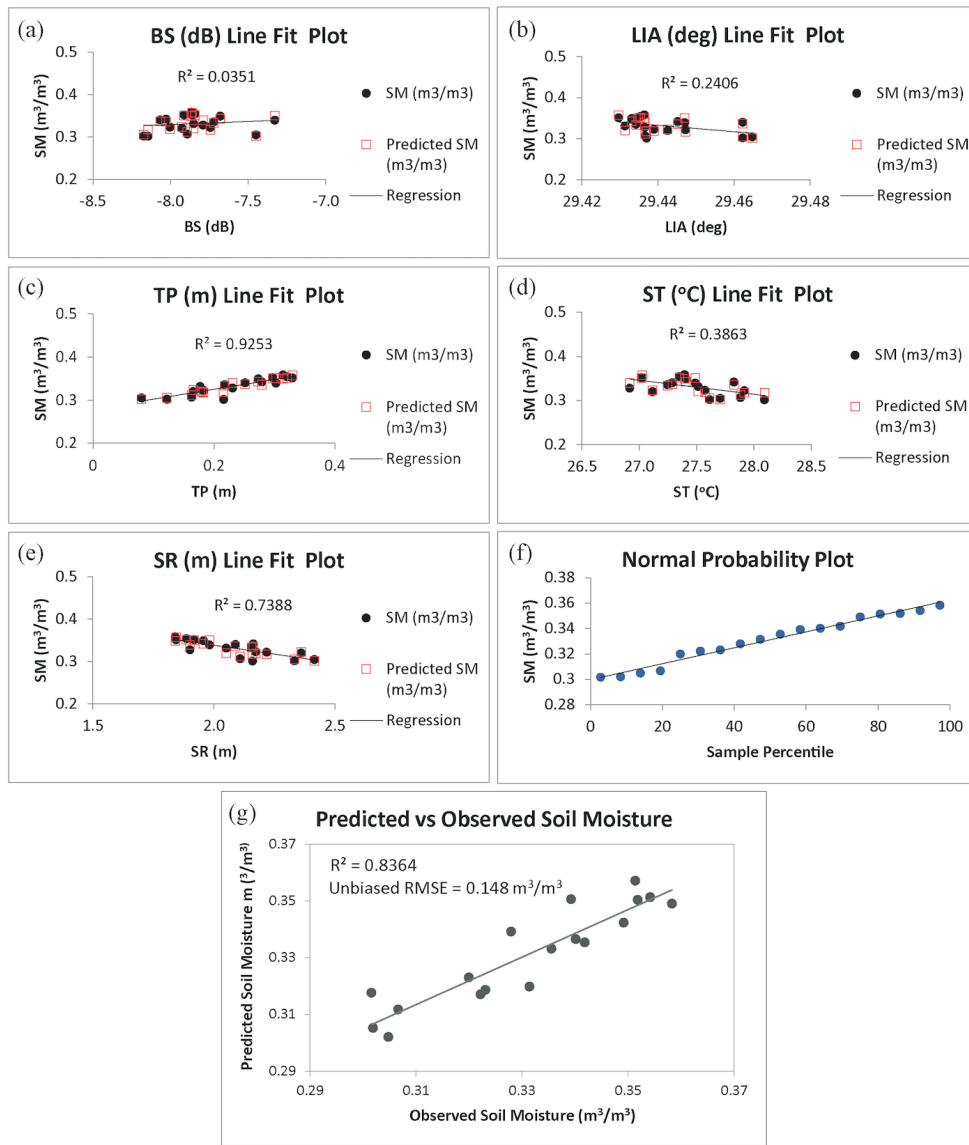


Fig. 2. (a-e) Linear regression fit plot among soil moisture and several variables used to derive a soil moisture equation; (f) Normal probability plot; (g) Correlation between predicted and observed soil moisture

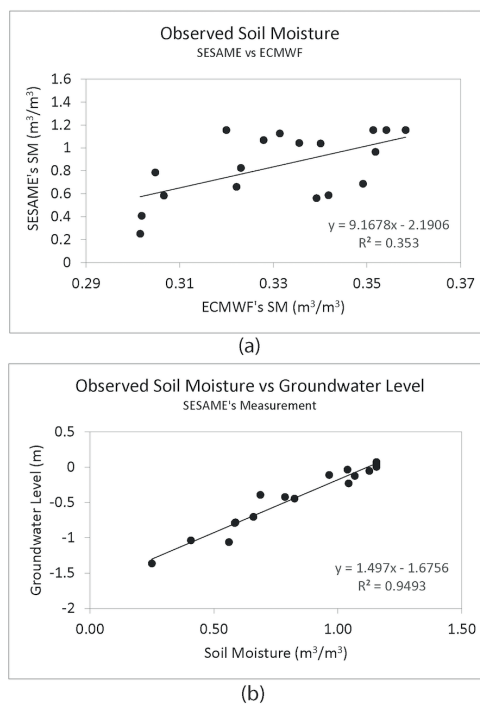


Fig. 3. Linear regression (a) between SESAME's and ECMWF soil moisture; (b) between SESAME's soil moisture and water level measurements

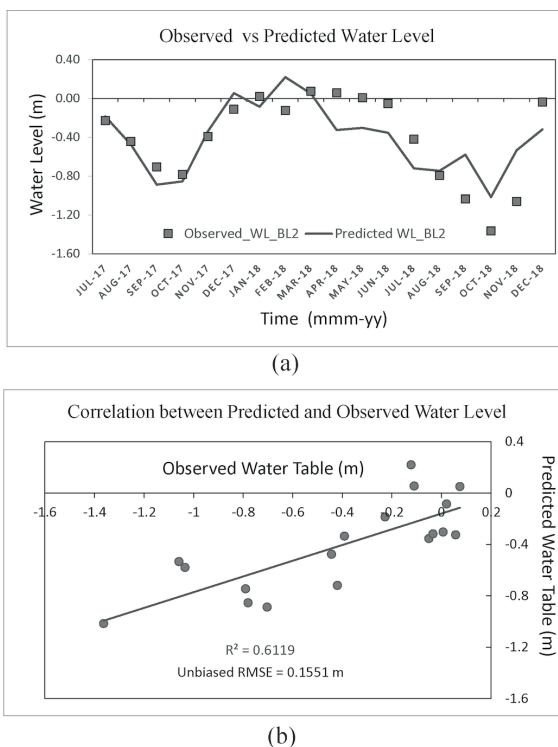


Fig. 4. Comparison between observed and predicted water levels at NBL2

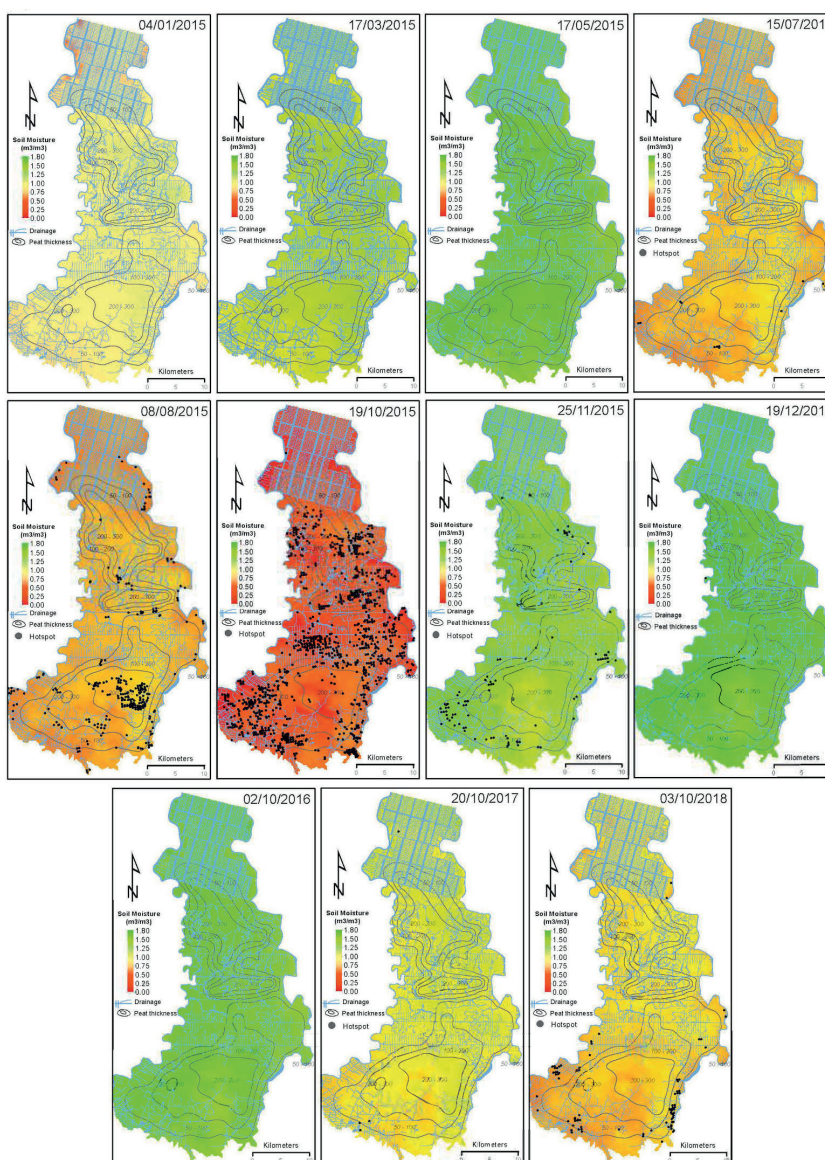


Fig. 5. Peat thickness (BBSDLP 2019) and drainage networks (Peat Restoration Agency 2017) overlaid on selected maps of spatiotemporal soil moisture from January 2015 to October 2018

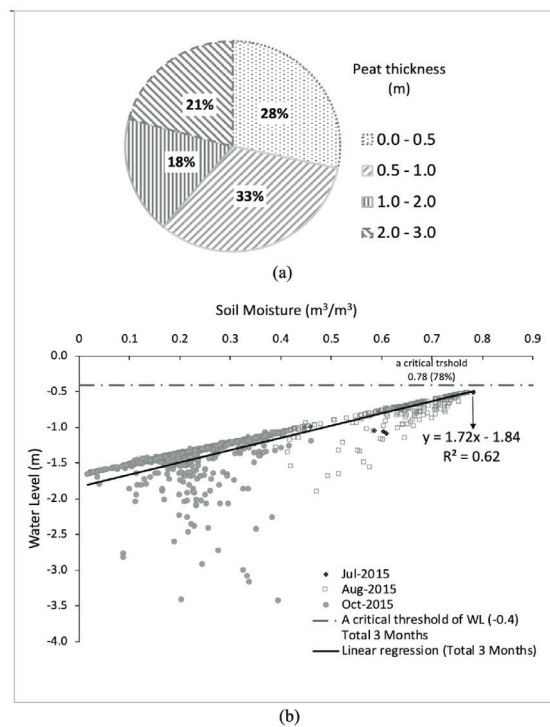


Fig. 6. Percentages of the number of hotspots associated with certain peat thickness; (b) relation between soil moisture and water levels at fire hotspot locations over the KHGSS site for July, August, and October 2015

Furthermore, the moisture content during 2016 – 2018 was generally higher than that in 2015. However, the moisture content continuously declined up to $\sim 0.25 \text{ m}^3\text{m}^{-3}$ during the dry season (around from July – October) for three consecutive years, 2016 - 2018. The lower soil moisture was associated with dense canal networks and around the edges of the KHGSS site, where two major rivers exist along its boundaries (Fig. 5). In addition, the spatial distribution of fire hotspots generally occurred in areas around these drainage networks, where most people living near the boundaries depend on the peatland for their livelihood including rice cultivation and oil palm plantation. Most of these areas have peat thickness in a range of 0 – 1 m with 61% of total hotspots, as shown in Fig. 6a.

Fig. 6b shows a relationship between variations of the soil moisture and water levels extracted from the point locations of the fire hotspots for July, August, and October 2015. Soil moisture was closely related to water levels, with a correlation of 0.65. Earlier fires, in July 2015, took place at higher moisture and shallower depth of groundwater level. Fig. 6b also indicates that moisture content of $0.78 \text{ m}^3\text{m}^{-3}$ (78%) and a groundwater level of $\sim 0.50 \text{ m}$ below peat surface represent the critical threshold for peat fires in the KHGSS.

Spatiotemporal groundwater level related to the critical threshold value

Fig. 7 shows that spatial variations of the groundwater levels tend to rise from January to May 2015, and most of the KHGSS area was flooding. In contrast, the groundwater levels had dropped to $\sim 5.0 \text{ m}$ below the peat surface from July to October 2015. These levels significantly exceeded the critical threshold of 0.4 m below the peat surface (President of Republic of Indonesia 2016b; Usup et al. 2004; Wösten et al. 2008).

Lower levels of groundwater occurred not only in the cultivation areas but also in the conservation area. In addition, the low amount of precipitation during these months was also responsible for large declines in the water level and soil moisture content. As a consequence, the peat became more susceptible to severe fires during the

dry season. Moreover, the peat surface elevation may also be lowering by several meters during this season (Khakim et al. 2020). Therefore, when the rainy season with large precipitation events, flooding occurred over this site area.

Although flooding of more than 1 m occurred over only a small area, 0.46% of this site in January 2016, the groundwater levels declined up to less than 0.4 m below the peat surface in the rainy season of the year 2017 and 2018 (Fig. 8). On the other hand, during the dry season from June to October, the groundwater levels over 30.5 – 99.0% of the site area dropped down to $\sim 0.7 \text{ m}$ below the peat surface.

Variations of groundwater levels with topographic features and drainage networks

Fig. 9 shows the profiles illustrating trends of estimated water levels varying with topographic elevations along transects 1 and 2 in 2015. The water levels were above the surface along transects 1 and 2 in the wet season (May and November), except in a peat dome area at the distance of $\sim 18 \text{ km}$ in transect 1. In contrast, they were below the surface in the dry season (July, August, and October).

Besides the seasons, topographic profiles influenced spatial variations of water level trends. The trends of the water level between these seasons were in opposite slope gradients. During the dry season, the groundwater trends varied relatively following the topographic profiles for lines 1 and 2. As the topography along line 2 has relatively flatter features and a narrower dome than that along line 1, the profiles of the water levels are relatively lower slope gradient along line 2 in May. Otherwise, slight downslope trends from the left to the right side of the profiles in November.

Furthermore, local trends of the fluctuations of the groundwater levels depended on the drainage systems, such as rivers and anthropogenic canals. The depth water table drawdown proximal to drainage and sensitive to local topography was performed in the study as presented in other areas of the shallow degraded peatland in the southwest of England (Luscombe et al. 2016) and of a fen

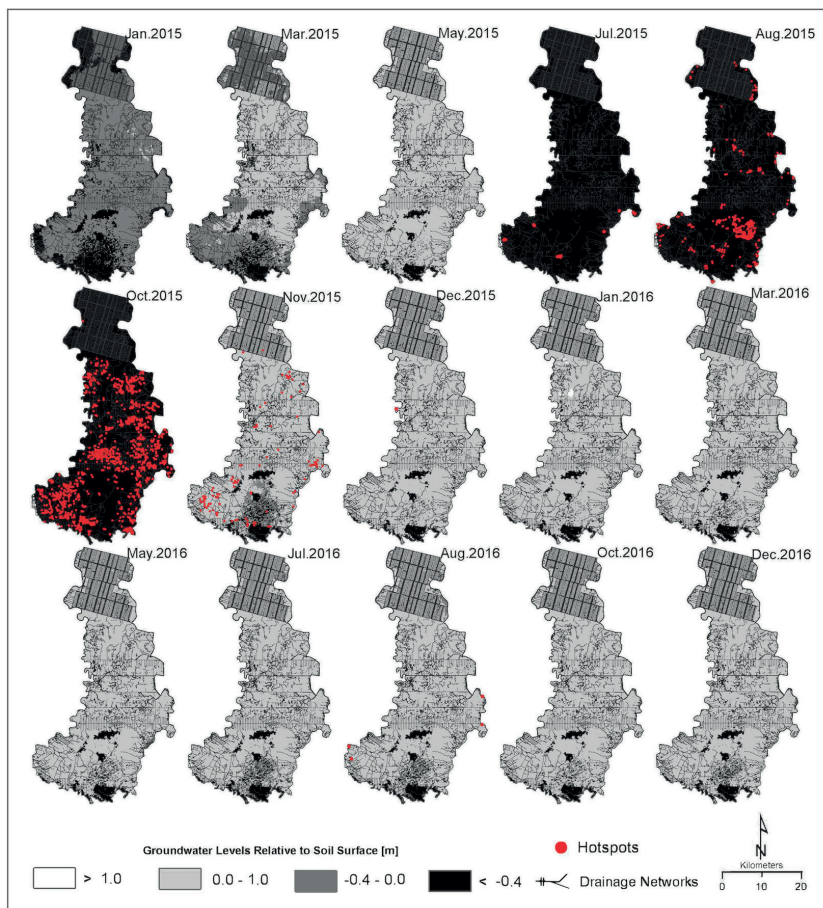


Fig. 7. Spatiotemporal variation of groundwater levels related to the critical threshold values for the year 2015–2016

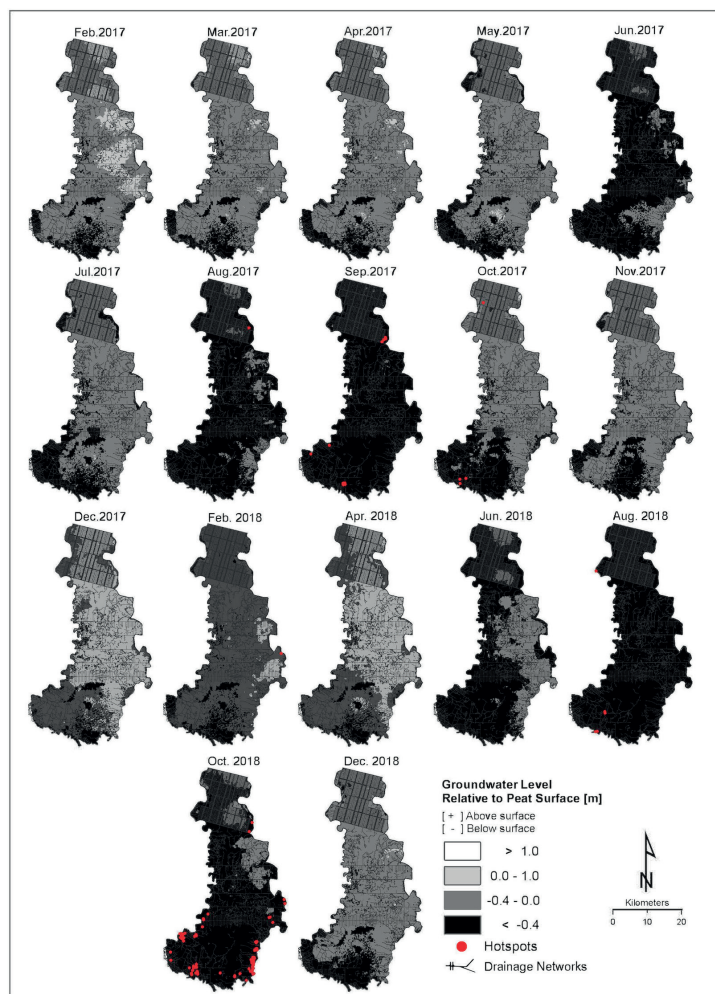


Fig. 8. Spatiotemporal variation of groundwater levels related to the critical threshold values for the year 2017–2018

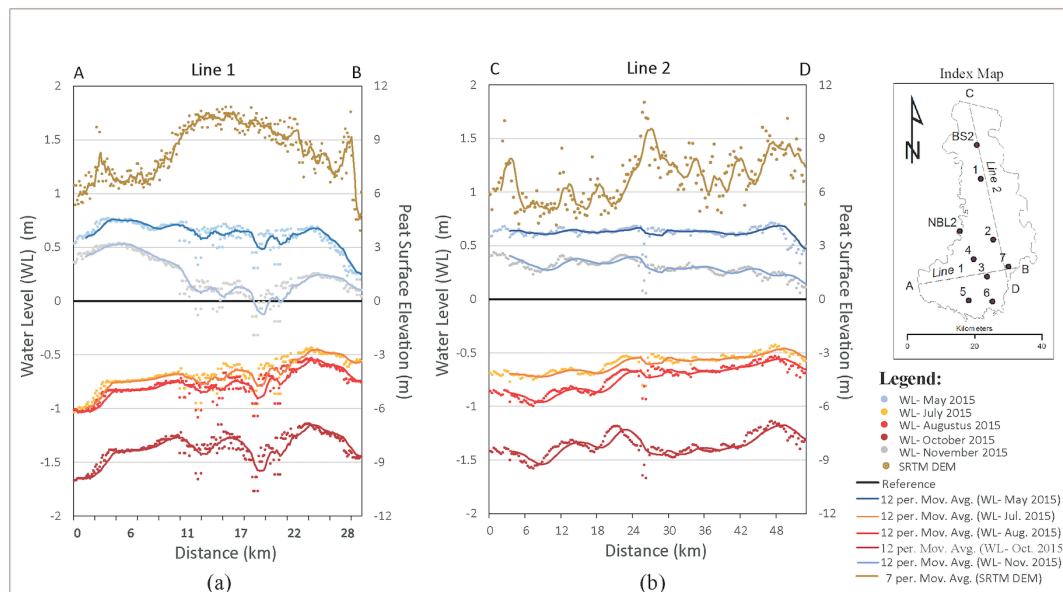


Fig. 9. Profiles of water level variations with topographic features along lines 1 (A-B) and 2 (C-D)

peatland near Quebec City (Whittington and Price 2006). The steepest gradient of the trends occurred on both sides of profile 1 and the right side of profile 2 due to the main rivers, i.e., Air Sugihan river and Air Saleh river. Therefore, higher variability of the groundwater levels between two seasons occurred in areas close to the main rivers. The trends due to drainage systems led to much amount of water discharged fast from a peatland in dry season (Khakim et al. 2020). Small fluctuations of the profiles may be associated with the anthropogenic canals.

Cause and effect relationship on groundwater level variations

Fig. 10 presents an interrelationship on several variables, including monthly precipitation, groundwater level, soil moisture, hotspots at nine points over the site area, and percentages of the areal extent of groundwater depths from 2015 to 2018. The predicted groundwater levels and moisture contents are commonly correlated to those from SESAME measurements.

The variations among the three first variables at all points during this period are highly correlated. The groundwater level and soil moisture also varied with monthly precipitation for seven selected locations from January 2015 to December 2018. Dramatical declines in monthly precipitations led to sharp decreases in groundwater levels from July to October 2015. Areal extent associated with the groundwater level less than the critical threshold of 0.4 m reached a maximum this month during the study period. This led to the much lower moisture content of the peat. Therefore, severe fires indicated by the number of hotspots occurred in October 2015.

In contrast, monthly precipitation increased after October 2015 and reached a peak in January 2016. Therefore, the groundwater levels, as well as the soil moisture content, increased. However, after this month, the groundwater level and soil moisture content gradually decreased and reached a minimum value in September 2017 and August 2018. The peat fires mostly occurred in cultivation and agriculture areas in October 2018. The number of hotspots in these months was much less than those in October 2015. This indicates that the fire hotspots did not occur when the groundwater levels were shallower than the threshold of 0.4 m. The fires occurred when the groundwater levels were deeper than the threshold.

DISCUSSION

The degraded peatland of KHGSS in South Sumatra is a restoration target area in Indonesia. Extensive drainage networks of the peatland area increased their vulnerability to fire, which was further enhanced by prolonged drought periods induced by the 2015 El Niño event. The amount of rainfall and the speed of water runoff influence the peatland catchment hydrology. Under natural conditions, the water table is close to or above the surface (Page et al. 2009). However, activities of illegal logging and land clearing for cultivation significantly impair the peatland holding water capacity in the site area. This condition led to dramatically decline in the water levels from July to October 2015. As a consequence, the peat was decomposed, and the groundwater level and moisture content were reduced. Furthermore, the moisture reduction had initiated subsurface fire to the self-heating and spontaneous combustion of dry peat. Therefore, a large number of hotspots were observed in 2015.

A minimum moisture content of the peat surface in the study area was predicted as much as $\sim 0.78 \text{ m}^3\text{m}^{-3}$ to preserve peat smoldering and it was corresponding to the groundwater depth of $\sim 0.5 \text{ m}$. It means 0.1 m deeper than the threshold that the Indonesia Government applies through Regulation No 57 of 2016 Concerning Amendment to Government Regulation No 71 of 2014 Concerning Peatland Ecosystem Protection and Management (President of Republic of Indonesia 2014, 2016b). This critical moisture content for peat smoldering varies according to peat types, such as 57-102% moisture for the National Park Service's Whiskeytown National Recreation Area, California, USA (Garlough and Keyes 2011). Peat with a bulk density of 150 kg m^{-3} could self-sustain smoldering propagation up to a critical moisture content of 115% (Prat-Guitart et al. 2016).

Rewetting is a hydrological restoration approach to maintain the groundwater level close to the peat surface. Groundwater is important in preserving the peat from carbon mineralization, peat degradation, and dehydration. The BRG has implemented restoration by blocking canals to rewet peatland over the study area in order to restore the pre-existing hydrological regime. Monitoring both the soil moisture and groundwater levels is the most important role in assessing the restoration efforts of the hydrological functions developed by the BRG based on rewetting activities.

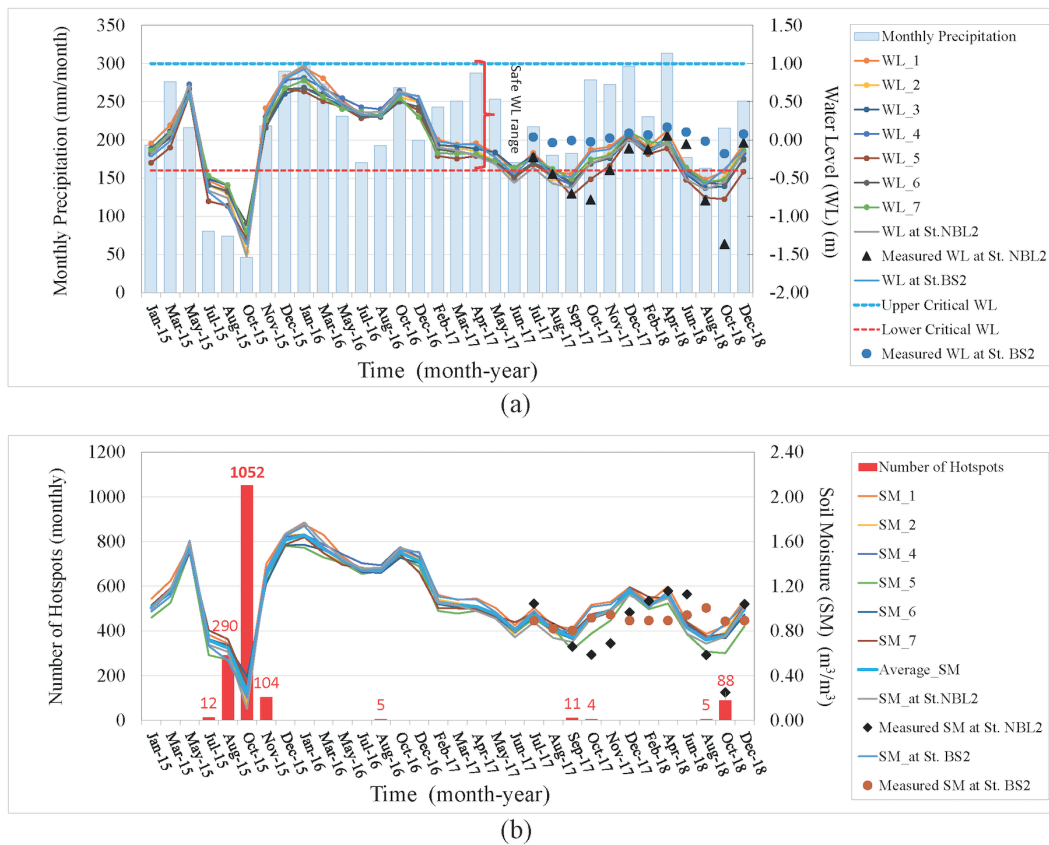


Fig. 10. Profiles of temporal variations of predicted and measured: (a) water levels with monthly precipitation and (b) soil moisture with a number of hotspots for 7 selected locations and 2 SESAME stations from January 2015 to December 2018

As rainfall was high in early 2016, the groundwater level and soil moisture content increased over the study area. However, combustion can create sub-surface hollows at several places within the peatlands (Roy et al. 2014). Thus, volume reduction associated with peat fires and water table depletion led to peatland subsidence (Khakim et al. 2020). The subsidence, in turn, induced flooding in the site area in January 2016. Nevertheless, the groundwater levels significantly dropped more than the critical threshold during the dry season (June–October) of the years 2017 and 2018. Thus, a few fires still occurred at the edge of the southern study area especially in October 2017 and 2018. Human activity is indicated as a main factor of these fires. Land use without regard to environmental sustainability, including illegal logging, canal construction, and plantation and agricultural development are activities that are still frequently carried out by people living near peatlands. Therefore, the restoration efforts became ineffectively in preventing the peat fires.

Furthermore, although the hydrological restoration by blocking canals has an advantage, which remains waterways passable for small boats for transportation of local communities, the canal blocking requires lots of large timber, easily damaged by persons wanting to re-open waterways, and not leading to full rewetting because of the spillways. For restoration to be more effective, comprehensive efforts need to be made to create other types of peatland rewetting and consistent law enforcement.

CONCLUSIONS

Soil moisture and water level dynamics in the KHGSS site have been successfully characterized using MRA analysis based on Sentinel-1 and ECMWF datasets. The estimated moisture contents and water levels agreed well with SESAME measurements. A minimum moisture content of peat smoldering combustion for this site can be indicated as much as $\sim 0.78 \text{ m}^3\text{m}^{-3}$ (78%), corresponding with a minimum water level of $\sim 0.50 \text{ m}$ below peat. The 2015 extreme drought and human activities such as illegal logging, land clearing, and canal construction impaired the water capacity of the peatland. Thus, the peatland ineffectively maintained the groundwater levels shallower than the threshold value (i.e., 0.4 m deep from the peat surface) in the dry season. The peat fires severely burned both cultivation and protected areas having dense catastrophic canals and closing to rivers. Furthermore, trends in groundwater levels and moisture contents increased in 2016. However, they gradually declined to reach $\sim 0.70 \text{ m}$ and $\sim 0.25 \text{ m}^3\text{m}^{-3}$, respectively, during the period of 2017 – 2018. Consequently, a few fires occurred during the dry season these years. We suggest that this area needs efforts to restore groundwater levels shallower than the threshold of 0.40 m along with law enforcement.

REFERENCES

- Asmuß T., Bechtold M. and Tiemeyer B. (2019). On the Potential of Sentinel-1 for High Resolution Monitoring of Water Table Dynamics in Grasslands on Organic Soils. *Remote Sensing*, 11(14), 1659, DOI: 10.3390/rs11141659.
- Attema E., Davidson M., Floury N., Levrini G., Rosich B., Rommen B. and Snoeij P. (2008). Sentinel-1 ESA's new European radar observatory. *Proceedings of the European Conference on Synthetic Aperture Radar, EUSAR*, 1-4, 2-4.
- Aukema J. and Wilson S. (2019). *THE SAR HANDBOOK: Comprehensive Methodologies for Forest Monitoring and Biomass Estimation*, A.I. Flores-Anderson, K.E. Herndon, R.B. Thapa & E. Cherrington eds.; First, DOI: 10.25966/nr2c-s697.
- Baghdadi N., Choker M., Zribi M., El Hajj M., Paloscia S., Verhoest N.E.C., Lievens H., Baup F. and Mattia F. (2016). A new empirical model for radar scattering from bare soil surfaces. *Remote Sensing*, 8(11), 1-14, DOI: 10.3390/rs8110920.
- BBSDLP. (2019). Map of Peatland of Sumatra Island, Scale 1:50,000.
- Chen Y., Qiao S., Zhang G., Xu Y.J., Chen L. and Wu L. (2020). Investigating the potential use of Sentinel-1 data for monitoring wetland water level changes in China's Momoge National Nature Reserve. *PeerJ*, 2020(2), 1-24, DOI: 10.7717/peerj.8616.
- Dabrowska-Zielinska K., Budzynska M., Tomaszewska M., Malinska A., Gatkowska M., Bartold M. and Malek I. (2016). Assessment of carbon flux and soil moisture in wetlands applying Sentinel-1 data. *Remote Sensing*, 8(9), DOI: 10.3390/rs8090756.
- Dabrowska-Zielinska K., Musial J., Malinska A., Budzynska M., Gurdak R., Kiryla W., Bartold M. and Grzybowski P. (2018). Soil moisture in the Biebrza Wetlands retrieved from Sentinel-1 imagery. *Remote Sensing*, 10(12), DOI: 10.3390/rs10121979.
- Dee D.P., Uppala S.M., Simmons A.J., Berrisford P., Poli P., Kobayashi S., Andrae U., Balmaseda M.A., Balsamo G., Bauer P., Bechtold P., Beljaars A.C.M., van de Berg L., Bidlot J., Bormann N., Delsol C., Dragani R., Fuentes M., Geer A.J., ... Vitart F. (2011). The ERA-Interim reanalysis: Configuration and performance of the data assimilation system. *Quarterly Journal of the Royal Meteorological Society*, 137(656), 553-597, DOI: 10.1002/qj.828.
- Dohong A. (2019). Restoring Degraded Peatland in Indonesia: the 3R Approach. PARISH F., YAN L.S., ZAINUDDIN M.F. & GIESEN W. (Eds.) *RSPO Manual on Best Management Practices (BMPs) for Management and Rehabilitation of Peatlands*. 2 Ed. Kuala Lumpur: RSPO., 57, 2016-2017.
- Dubois P.C., Zyl J. V and Engman T. (1995). Measuring soil moisture with imaging radars. *IEEE Transactions on Geoscience and Remote Sensing*, 33(4), 915-926, DOI: 10.1155/2015/610307.
- Evers S., Yule C.M., Padfield R., O'Reilly P. and Varkkey H. (2017). Keep wetlands wet: the myth of sustainable development of tropical peatlands – implications for policies and management. *Global Change Biology*, 23(2), 534-549, DOI: 10.1111/gcb.13422.
- Filippini F. (2019). Sentinel-1 GRD Preprocessing Workflow. *Proceedings*, 18(1), 11, DOI: 10.3390/ecrs-3-06201.
- Gangat R., van Deventer H., Naidoo L. and Adam E. (2020). Estimating soil moisture using Sentinel-1 and Sentinel-2 sensors for dryland and palustrine wetland areas. *South African Journal of Science*, 116(8), 1-9, DOI: 10.17159/sajs.2020/6535.
- Garlough E.C. and Keyes C.R. (2011). Influences of moisture content, mineral content and bulk density on smouldering combustion of ponderosa pine duff mounds. *International Journal of Wildland Fire*, 20(4), 589-596, DOI: 10.1071/WF10048.
- Giesen W. and Sari E.N.N. (2018). Tropical Peatland Restoration Report : the Indonesian case Tropical Peatland Restoration Report : The Indonesian Case Berbak Green Prosperity Partnership/Kemitraan Kesejateraan Hijau (Kehijau Berbak), Issue March, DOI: 10.13140/RG.2.2.30049.40808.
- Hooijer A., Page S., Canadell J.G., Silvius M., Kwadijk J., Wösten H. and Jauhiainen J. (2010). Current and future CO₂ emissions from drained peatlands in Southeast Asia. *Biogeosciences*, 7(5), 1505-1514, DOI: 10.5194/bg-7-1505-2010.
- Hooijer A., Silvius M., Wosten H. and Page S. (2006). PEAT-CO₂, Assessment of CO₂ Emissions From Drained Peatland in SE Asia. [http://www.wetlands.org/Portals/0/publications/Report/Peat CO2 report.pdf](http://www.wetlands.org/Portals/0/publications/Report/Peat_CO2_report.pdf)
- Hooijer Aljosja, Silvius M., Wösten H., Page S., Hooijer A., Silvius M., Wösten H. and Page S. (2006). PEAT-CO₂, Assessment of CO₂ emissions from drained peatlands in SE Asia. *Delft Hydraulics Report Q3943*, 36.
- Hornáček M., Wagner W., Sabel D., Truong H., Snoeij P., Hahmann T., Diedrich E. and Doubkova M. (2012). Potential for high resolution systematic global surface soil moisture retrieval via change detection using Sentinel-1. *IEEE Journal of Selected Topics in Applied Earth Observations and Remote Sensing*, 5(4), 1303-1311, DOI: 10.1109/JSTARS.2012.2190136.
- Khakim M.Y.N., Bama A.A., Yustian I., Poerwono P., Tsuji T. and Matsuoka T. (2020). Peatland subsidence and vegetation cover degradation as impacts of the 2015 El Niño event revealed by Sentinel-1A SAR data. *International Journal of Applied Earth Observation and Geoinformation*, 84(August 2019), DOI: 10.1016/j.jag.2019.101953.
- Kim J.W., Lu Z., Gutenberg L. and Zhu Z. (2017). Characterizing hydrologic changes of the Great Dismal Swamp using SAR/InSAR. *Remote Sensing of Environment*, 198, 187-202, DOI: 10.1016/j.rse.2017.06.009.
- Lee J. Sen. (1981). Speckle analysis and smoothing of synthetic aperture radar images. *Computer Graphics and Image Processing*, 17(1), 24-32, DOI: 10.1016/S0146-664X(81)80005-6.
- Leng L.Y., Ahmed O.H. and Jalloh M.B. (2019). Brief review on climate change and tropical peatlands. *Geoscience Frontiers*, 10(2), 373-380, DOI: 10.1016/j.gsf.2017.12.018.
- Li J., Wang S., Gunn G., Joosse P. and Russell H.A.J. (2018). A model for downscaling SMOS soil moisture using Sentinel-1 SAR data. *International Journal of Applied Earth Observation and Geoinformation*, 72(May), 109-121, DOI: 10.1016/j.jag.2018.07.012.
- Luscombe D.J., Anderson K., Grand-Clement E., Gatis N., Ashe J., Benaud P., Smith D. and Brazier R.E. (2016). How does drainage alter the hydrology of shallow degraded peatlands across multiple spatial scales? *Journal of Hydrology*, 541, 1329-1339, DOI: 10.1016/j.jhydrol.2016.08.037.
- Miettinen J., Wang J., Hooijer A. and Liew S. (2013). Peatland Conversion and Degradation Processes in Insular Southeast Asia: a Case Study in Jambi, Indonesia. *Land Degradation & Development*, 24(4), 334-341, DOI: 10.1002/ldr.1130.
- Oh Y., Sarabandi K. and Ulaby F.T. (1992). An empirical model and an inversion technique for radar scattering from bare soil surface. *IEEE Transactions on Geoscience and Remote Sensing*, 30(2), 370-381.
- Page S., Hoscio A., Wösten H., Jauhiainen J., Silvius M., Rieley J., Ritzema H., Tansey K., Graham L., Vasander H. and Limin S. (2009). Restoration ecology of lowland tropical peatlands in Southeast Asia: Current knowledge and future research directions. *Ecosystems*, 12(6), 888-905, DOI: 10.1007/s10021-008-9216-2.
- Peat Restoration Agency. (2017). Final Report: Data Acquisition and Thematic Mapping in KHG Area of Cawang - Lalang River and KHG of Sugihan - Saleh River.

- Prat-Guitart N., Rein G., Hadden R.M., Belcher C.M. and Yearsley J.M. (2016). Propagation probability and spread rates of self-sustained smouldering fires under controlled moisture content and bulk density conditions. *International Journal of Wildland Fire*, 25(4), 456-465, DOI: 10.1071/WF15103.
- Protection and management of the peat ecosystem, Pub. L., 71 (2014).
- Amendment to Government Regulation Number 71 of 2014 concerning peatland ecosystem protection and management, Pub. L. No. 57 (2016).
- Peat Restoration Agency, Pub. L., 1 (2016).
- Republic of Indonesia. (2018). Project final report between JICA (Japan International Cooperation Agency) and BRG (Peatland Restoration Agency in Indonesia).
- Roy P.D., Rivero-Navarrete A., Sánchez-Zavala J.L. and López-Balbiaux N. (2014). Subsurface fire and subsidence at Valle del Potosí (Nuevo León, Mexico): Preliminary observations. *Boletín de La Sociedad Geológica Mexicana*, 66(3), 553-557, DOI: 10.18268/BSGM2014v66n3a10.
- Schroeder W., Oliva P., Giglio L. and Csiszar I.A. (2014). The New VIIRS 375m active fire detection data product: Algorithm description and initial assessment. *Remote Sensing of Environment*, 143, 85-96, DOI: 10.1016/j.rse.2013.12.008.
- Sodikin E., Munandar M., Setiawan A., Prayitno M.B. and Suwandi S. (2017). Pilot project implementasi paludikultur dan agroforestry lahan APL di Desa Perigi, Pangkalan Lampam, KHG Sungai Sugihan - Saleh Lumpur Ogan Komering Ilir, Sumatera Selatan.
- Sulaiman A., Sari E.N.N. and Saad A. (2017). Panduan teknis pemantauan tinggi muka air lahan gambut sistem telemetri. The Republic of Indonesia Peat Restoration Agency.
- Usup A., Hashimoto Y., Takahashi H. and Hayasaka H. (2004). The principal types of vegetation in the Tropics, 14(1), 1-19. https://www.jstage.jst.go.jp/article/tropics/14/1/14_1_1/_pdf
- Whittington P.N. and Price J.S. (2006). Advanced Bash-Scripting Guide An in-depth exploration of the art of shell scripting Table of Contents. *Hydrological Processes*, 20, 3589-3600, DOI: 10.1002/hyp.6376.
- Wösten J.H.M., Clymans E., Page S.E., Rieley J.O. and Limin S.H. (2008). Peat-water interrelationships in a tropical peatland ecosystem in Southeast Asia. *Catena*, 73(2), 212-224, DOI: 10.1016/j.catena.2007.07.010.
- Wösten J.H.M., Van Den Berg J., Van Eijk P., Gevers G.J.M., Giesen W.B.J.T., Hooijer A., Idris A., Leenman P.H., Rais D.S., Siderius C., Silviu M.J., Suryadiputra N. and Wibisono I.T. (2006). Interrelationships between hydrology and ecology in fire degraded tropical peat swamp forests. *International Journal of Water Resources Development*, 22(1), 157-174, DOI: 10.1080/07900620500405973.
- Zhang Xianlong, Chan N.W., Pan B., Ge X. and Yang H. (2021). Mapping flood by the object-based method using backscattering coefficient and interference coherence of Sentinel-1 time series. *Science of the Total Environment*, 794, 148388, DOI: 10.1016/j.scitotenv.2021.148388
- Zhang Xuefei, Zhang T., Zhou P., Shao Y. and Gao S. (2017). Validation analysis of SMAP and AMSR2 soil moisture products over the United States using ground-based measurements. *Remote Sensing*, 9(2), DOI: 10.3390/rs9020104.